USE OF PROPAGATION CORRECTIONS FOR VLF TIMING

Eric R. Swanson

Naval Electronics Laboratory Center

ABSTRACT

The theory of VLF timing from phase measurements is briefly reviewed with attention to both frequency and epoch. Propagational aspects are noted without specific attention to predictional details. "Cycle slippage" is described. Application of propagation corrections to VLF timing is described, with particular attention to the use of available sky-wave corrections published for the OMEGA Navigation System.

INTRODUCTION

The past, present, and future of VLF time dissemination has recently been described simplistically as time ticks, frequency comparison, and total epoch dissemination, respectively. (1) Throughout the past decade, phase comparisions at VLF have been in general use as a method of frequency intercomparison of precision oscillators. Typically, such comparisons are made between fixed sites and at the same times of day so that phase predictions are relatively unimportant often the "prediction" simply being the assumption that seasonal and diurnal variations are not important. Foreseen in the future is increased use of VLF for epoch dissemination as has been used over the past six years to hold the intercontinental OMEGA navigation stations in synchronization to within a few microseconds. For epoch dissemination to sites without calibration by flying clock or other ancillary means, propagation predictions will be necessary. In addition, the use of propagation corrections can improve the accuracy of frequency or epoch determination and increase flexibility through allowing signal comparison at any hour of the day.

VLF PHASE

General

A recent review of VLF timing is given in Reference 1 while a fundamental tutorial discussion of the nature of the measurement will be found in Reference 2. Briefly, we wish to compare two remote clocks. Since frequency is the derivative of phase (expressed in cycles), only the ability to disseminate epoch need be considered in order to establish capabilities for dissemination of frequency. A stabilized transmitter is assumed as the source of standard continuous wave (CW) signals of fixed frequency and known epoch. A similar frequency is derived locally at a remote site and the phase is shifted until it is in coincidence (or quadrature) with the received signal. The amount of shift is related to time by the association that one cycle of phase shift corresponds to the time represented by one period of the CW signal. The absolute shift required after allowance for propagation can be related to the epoch of the local clock. Any variation in the shift apart from

propagational changes may be associated with a frequency offset between the local oscillator and transmitter standard reference.

The repeatability and stability of VLF signal propagation has long been recognized. Figure 1 shows the average phase of Haiku, Hawaii, received in New York. Although the diurnal variation corresponds to about 100 μs (1 centicycle (ccc) at 10.2 kHz $\approx$ 1 μs), the hourly standard deviation was only about 2 μs. The most common applied "predictions" for timing are probably that the phase is repeatable from day to day when examined at the same time or that phase is time independent or "flat" during the night or nearly midday (0800 and 2100 in Figure 1). In practice, the latter assumption is more nearly satisfied near 20 kHz and above rather than at 10.2 kHz, which typically exhibits a slow diurnal "curvature" during the day as shown in the figure.

Although experimental, the variation shown in Figure 1 is typical in the classical sense of being most representative of an ideal rather than being common or expected. Four main regions may be identified. Constant phase is observed from about 0600 to 0900Z when the entire propagation path is dark. This period is identified propagationally as night. Sunrise at the New York end of the path occurred near 0900Z and the phase proceeded into a ramping decrease as sunrise proceeded on path to Hawaii. About 1600, sunrise occurred in Hawaii and the phase then stabilized to a nearly constant daytime value continuing a slight decrease until noon, due to variation in the solar zenith angle. The sunset process is essentially the reverse of the sunrise process. The behavior described is expected most at the VLF navigational frequencies (10-14 kHz) over long east-west paths. Several complexities generally need to be considered. The illustration shows a situation in which propagation may be associated with only one earth-ionosphere waveguide propagation mode. Even in such a relatively simple case, some complexity is expected due to ionospheric time constants resulting in a slight lag between the nominal VLF phase variation and the zenith angle variation and an abrupt phase change presumably associated with photo detachment at sunrise. The complexities inherent even to a propagation model employing only a single propagation mode are described in detail for 10.2
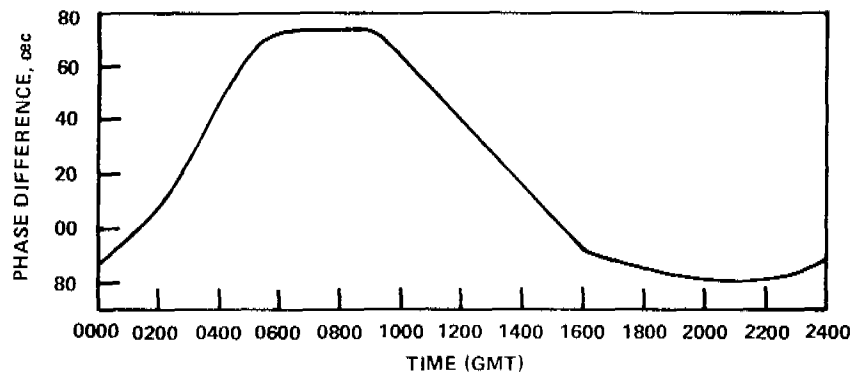

Figure 1. Average 10.2-kHz phase of Haiku, Hawaii, received at Forestport, New York, station, May 17-24, 1966. Standard deviation approximately 2 ccc.

kHz by Swanson and Bradford and are more apparent on measurements over north-south paths (3). Especially above 2 kHz, multimode propagation may be important as is described in the subsequent section. It is also possible that modal conversion may occur at the sunrise or sunset terminators wherein some propagation by the first waveguide mode may be converted into the second waveguide mode or conversely. (4, 5)

Modal Variation

When two or more propagation modes are effective, the received signal will be the phasor sum of the components. Maximum and rms phase irregularity from the interference of two waveguide modes of various amplitudes have been computed by Gallenberger and are given in Reference 6. Provided one mode remains dominant, the phase irregularity will be less than quadrature; thus corresponding to a variation of 25 microseconds at 10 kHz and about eight microseconds at 30 kHz. Even with a nominal "dominance" of 5 dB, the maximum phase variations will correspond to less than ten microseconds. Typically, the first mode will be dominant by considerably more than 5 dB over long paths during the day. However, without detailed specific computation for the path considered, it is not clear what mode will be dominant at night, especially above 20 kHz. Unless the same mode is dominant throughout the 24-hour day, a phenomenon referred to as "cycle slipping" or "cycle jumps" can occur.

Cycle slippage should not be confused with failure to maintain proper phase tracking due to reduced signal. Although it is true that an amplitude minimum will usually correspond to the cycle slip, the minimum may still be quite sufficient that the receiving equipment track properly. Essentially, if modal dominance changes between day and night, then it is self-evident that the modes must be equal somewhere during sunrise and sunset transitions. The important consideration is then what the relative phase of the two modes is at equality. If the modes are in phase, then the field strength is enhanced and no unusual variation is necessarily seen in amplitude. If they are in opposition, a null will occur; the signal will disappear and a receiver will necessarily attempt to track noise. More commonly, neither of these extremes will occur.

An example will help to illustrate the possibilities. Assume a first-mode diurnal phase change of one cycle. This may be illustrated as the locus of a vector of nearly constant or slightly increasing magnitude during sunset with relatively uniform phase shift as shown in Figure 2(a). As the diurnal change in velocity and amplitude of the second mode would usually be much greater, a possible locus for the second mode contribution is represented in Figure 2(b). The observed diurnal phase change will follow the locus of the phasor sum. Both the absolute phasing and the diurnal phase change on each mode can vary slightly from one day to the next as a function of random variations in the ionosphere. As a quantitative example, on a 5000-km path with propagation conditions comparable with isotropic propagation between San Diego and Hawaii, amplitude and phasing would be as indicated in Table 1.

(a) FIRST MODE (≈ 1 CYCLE)

(b) SECOND MODE (≈ 2 CYCLES)

Figure 2. Vector loci for modal variation during sunset transition.

Table 1

Hypothetical Amplitude Over a 5000-km Path.

Frequency	Diurnal Period	Mode	Amplitude Phase (relative dB)
10 kHz	Day	1	-13.5
		2	-93.8
	Night	1	-8.5
		2	-58.2
20 kHz	Day	1	-8.3
		2	-29.7
	Night	1	-14.0
		2	-16.0

Propagation constants from Wait & Spies, 70 km during the day[7]; Snyder and Pappert, 84 km at night[8].

During the day, single-mode propagation is closely approximated at either frequency. At night, single-mode propagation is closely approximated at 10 kHz while the modes are nearly equal at 20 kHz. Indeed, had a slightly shorter path been considered, the second mode would have dominated at night at 20 kHz. Nominal phase values based on isotropic ionospheres of 70 and 84 km day and night, respectively, are given in Table 2.

Table 2
Nominal Phase Values Over a 5000-km Path.

Frequency	Diurnal Period	Mode	Phase (Cycles With Respect to Ground Wave)
10 kHz	Day	1	-0.6
		2	-8.3
	Night	1	-0.1
		2	5.8
20 kHz	Day	1	0.6
		2	-3.3
	Night	1	1.2
		2	-1.7

The diurnal phase change is about 0.5 cycle on the first mode but about two cycles on the second. More important, the absolute phase being received is several cycles different between the modes. Thus, if the entire propagation path should suffer an anomalous height variation corresponding to one-tenth of the diurnal height change, the relative arrival phase of 10 kHz would advance or delay about five centicycles at any time during the 24-hour day, but the second mode would suffer an anomalous variation of about 0.1 (8.3 - 5.8) = 0.25 cycles. That is, the first mode phase would be only slightly changed while the second mode phase would be shifted to quadrature. The relative phase between the modes would thus be significantly altered as would the phasor sum. Thus, as the ionosphere varies slightly from day to day, the diurnal phase variation may change quite substantially if a change in modal dominance occurs between day and night. Considering the contribution of still other modes, the phasor sum locus may circle the origin once, twice, several times or not at all depending entirely on the relative phase relations of the various modes during transitions. This can lead to several types of anomalous phase shift. The diurnal pattern could be one full cycle more or less than nominal, or it could always gain a cycle at sunrise and lose one at sunset, or any of a nearly unlimited number of alternative possibilities might apply. Further, phase shift may not repeat from day to day. Detailed 24-hour prediction and reliable use of signals experiencing a change of modal dominance would thus depend on a very careful analysis. Reliable use would be possible only under unusual circumstances.

The cycle slip phenomena is illustrated in Figures 3, 4, and 5. In each case, the assumed model is that of two modes, each of which has constant phase and amplitude both day and night, but for which the amplitudes and phases vary uniformly through an assumed ramp sunrise or sunset transition. In each case, the diurnal variation was assumed to be one cycle on the first mode and two cycles on the second mode. Figure 3 shows hypothetical amplitude and phase variation when only the first mode is present. Figure 4 shows hypothetical variations when the first mode remains dominant. Figure 5 shows variations when modal dominance changes.

Signal Selection

The foregoing illustrates some forms of diurnal phase variations which may be observed in practice and emphasizes the difficulty of quantitative explanation of the entire 24-hour
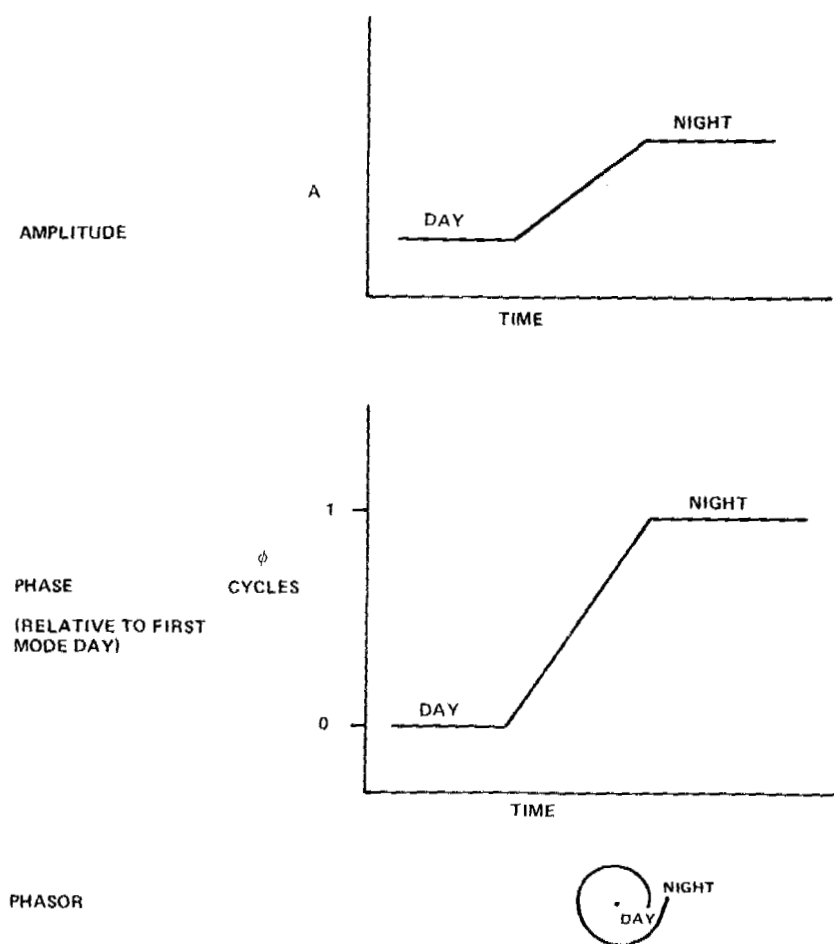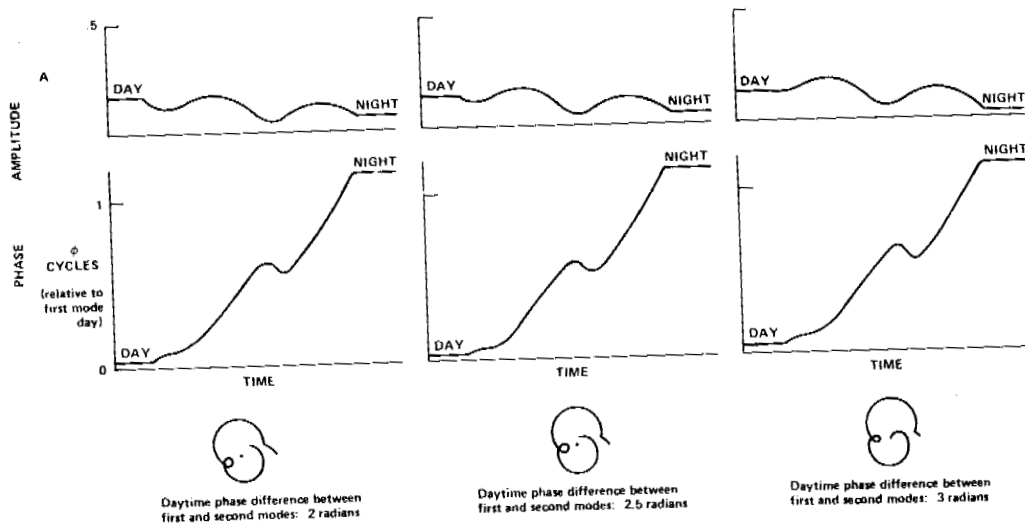

Figure 3. Sunset diurnal variation--first mode only.

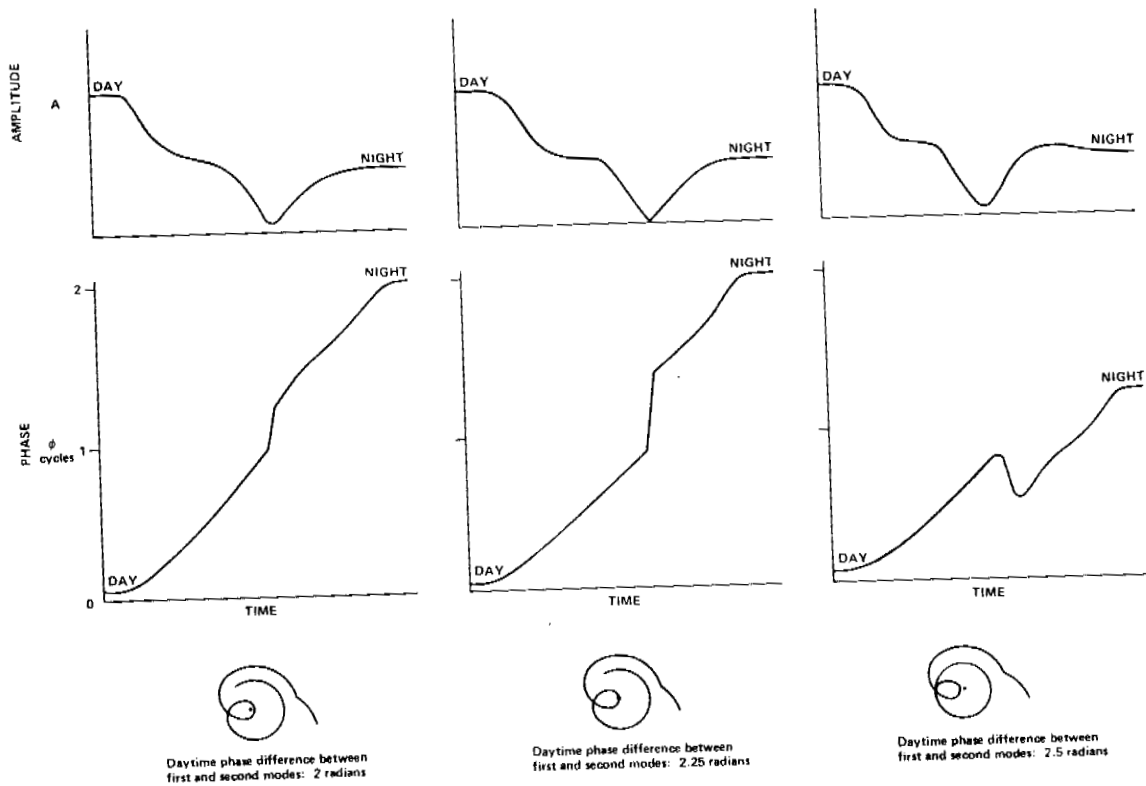Figure 4. Sunset diurnal variation–first and second modes, first mode dominant.

Figure 5. Sunset diurnal transition–first and second modes, change of mode dominance.

316

diurnal variation when modal dominance changes. Since phase repeatability may also be poor under conditions of competitive modes, the best solution in such cases is one of signal avoidance. In any conceivable location, many VLF signals will be available and it is unnecessary to attempt accurate time determinations using signals of inordinately complex structure. Signal selection is, however, a matter of considerable practical importance since, to many engineers, the best signal is the loudest—this is also likely from the closest station at the highest frequency and therefore, exhibiting the most complex structure. For the balance of this paper, the signal is assumed to be of essentially single mode character— at least during the diurnal period of observation. Signals propagated by more complex structures may also be used, but their calibration and potential seasonal variation are best obtained by ancilliary methods such as flying clock or by "boot-strap" wherein more predictable signals are used as a reference until sufficient statistical confidence is generated.

Uncertainty in the spatial prediction of phase also may be a factor in signal selection. Spatial prediction theory at the navigation frequencies is discussed in Reference 6 which shows the importance of a number of path parameters such as ground conductivity, path orientation, latitude and so forth to phase prediction. Prediction errors and signal selection at the OMEGA frequencies are discussed in detail in Appendices D and F of Reference 9. Desirable characteristics from the viewpoint of spatial resolution include daytime illumination, high ground conductivity such as sea water or normal land—and temperate latitude propagation.

Propagation Corrections and Application

Precise propagation corrections for VLF phase are presently published only for the 10.2 kHz OMEGA frequency. Necessary computational parameters for phase prediction at 13.6 and 11.33 kHz are available and normally used within multifrequency OMEGA receivers which compute propagation corrections internally. Tabular computation at 13.6 and 11.33 kHz is occasionally produced, but not published. Propagation predictions at 10.2 kHz are widely distributed by the Defense Mapping Agency (formerly Oceanographic Office) in the series H.O. Pub 224 *et seq.* available from clearing houses in Philadelphia, Pennsylvania, and Clearfield, Utah. The series includes various volumes depending on area. In the temperate latitudes, skywave corrections are computed for every four degrees of latitude and longitude.

A sample skywave correction table is shown in Figure 6. Phase corrections are tabulated hourly for semimonthly periods. The corrections are referred to as "0.9974 × ground-wave" geodetic reference, which is the circular OMEGA line of position defined by

$$G_R = \frac{0.9974\,d}{\lambda}$$

DATE								GMT									
	00	01	02	03	04	05	06	07	08	⋯	18	19	20	21	22	23	24
JAN 1–15	−71	−71	−71	−71	−71	−71	−71	−71	−71		−24	−40	−61	−71	−71	−71	−71
JAN 16–31	−71	−71	−71	−71	−71	−71	−71	−71	−68		−20	−36	−57	−71	−71	−71	−71
FEB 1–14	−71	−71	−71	−71	−71	−71	−71	−71	−59		−16	−31	−52	−71	−71	−71	−71
FEB 15–28	−71	−71	−71	−71	−71	−71	−71	−67	−44		− 9	−24	−45	−71	−71	−71	−71
MAR 1–15	−71	−71	−71	−71	−71	−71	−70	−59	−32		− 5	−17	−39	−70	−71	−71	−71
. . .																	
DEC 16–31	−71	−71	−71	−71	−71	−71	−71	−71	−71		−26	−43	−65	−71	−71	−71	−71

LOCATION 16°0′N 40°0′W
STATION A: NORWAY

Figure 6. Skywave correction table.

Referencing to the line of position removes most of the spatial variation. The most precise prediction can be obtained by interpolating from skywave corrections published for the four grid squares surrounding the receiving site. However, the published density of skywave corrections is sufficient that interpolation will only improve the predictions by five microseconds or less from assuming the nominal table for the grid square in which the receiver is located.

A detailed example of the application of skywave corrections to timing is given in Sample Procedure 1 below. A typical long-term calibration error day or night is 3.25 microseconds.

It is noteworthy that if absolute epoch is not important, the geodesic calculation can be disregarded. Hourly or semimonthly differences in the skywave corrections as tabulated are valid corrections for use in estimating nominal seasonal or diurnal propagational phase change to determine frequency.

The foregoing technique can be applied to any frequency within the navigation band by interpolating skywave corrections between computations for 10.2, 11.33, and 13.5 kHz. However, slight anomalous differences between frequencies, such as caused by modal interference when two or more modes are present, may be important when deducing propagation corrections for subsequent use in cycle determination. As an example, consider predictions at 12.0 and 12.250 kHz as might be used with the timing receiver described by Wilson, Britt, and Chi. (10) Assume interpolation of OMEGA predictions predicts both carriers to an average nominal accuracy of 3.25 microseconds, but produces a differential prediction error of two centicycles due to the presence of some second-mode contamination on the signals. Since the time associated with the differential phase prediction error on the difference frequency is referred to the difference frequency period, the error is now two centicyles referred to the four millisecond period of 250 Hz; that is, 80 microseconds. Viewed in this way, the error is gross and much too large to support

318

A.	PATH LENGTH	d	7772.487 km		
	WAVELENGTH	$\lambda_{13.6}$	22.04 km/cycle		
PREDICTED	REFERENCE PATH DELAY	G_R	$-0.9974\ d/\lambda_{13.6}$ kHz	-351.679 cycles	
	DIURNAL CORRECTION	SWC_R	published table	-0.950 cycles	
VALUES	E-FIELD PHASE	ϕ_{P_E}	$G_R + SWC_R$	-352.629 cycles	
	LOOP ANTENNA ADJUSTMENT	ϕ_A	¼ cycle, if applicable	+0.250 cycles	
	H-FIELD PHASE	ϕ_{P_H}	$\phi_{P_E} + \phi_A$	-352.379 cycles	-352.279 cycles

B.	MEASURED FRACTION	ϕ_O	$\phi_{REMOTE} - \phi_{LOCAL}$	-0.389 cycles	
OBSERVED	CYCLE IDENTIFICATION	ϕ_N	$\phi_{P_H} - \phi_O < 0.5$ cycle	-352.0 cycles	
VALUES	OBSERVED PHASE	ϕ_O	$\phi_O + \phi_N$	-352.389 cycles	-352.389 cycles

C. CLOCK PHASE	ERROR	E_ϕ	PREDICTED - OBSERVED, $\phi_{P_H} - \phi_O'$	+0.010 cycles
	AMBIGUITY	ϕ_T	CARRIER FREQUENCY CYCLES	±N cycles

C. CLOCK TIME	ERROR	E_T	$\dfrac{\text{PHASE}}{\text{FREQUENCY}}\ \dfrac{E_\phi}{f}$	+0.7 μs
	AMBIGUITY	t_T	CARRIER FREQUENCY PERIODS	±NT μs

Sample Procedure 1: phase epoch determination. Done for Hawaii signal observed at the Naval Observatory on 13.6 kHz on 112000Z November 1969 — loop antenna (refer to text on facing page).

A. PREDICTED VALUE CALCULATIONS

1. From the known propagation path length d and the wavelength λ of the specific carrier being observed, compute the reference path delay or geodesic G_R:

$$G_R = -0.9974 d / \lambda_f$$

2. Look up the expected diurnal correction SWC_R in a skywave correction table. Select the value for the appropriate transmitter, frequency, year, month, day, and fraction of an hour:

$$SWC_R = \text{tabulated values}$$

3. Add the reference path delay to the diurnal correction to compute the predicted phase for the E-field vector ϕ_{P_E}:

$$\phi_{P_E} = G_R + SWC_R$$

4. If a loop antenna is used to observe the H-field vector, *reduce* the predicted E-field delay by ¼ cycle to compensate for the 90° lag of the E-field from the H-field:

$$\phi_{P_H} = \phi_{P_E} + 0.25$$

B. OBSERVED VALUE CALCULATIONS

1. Record the measured fractional cycle delay ϕ_O of the remote versus the local phase:

$$\phi_O = \phi_R - \phi_L) = \text{data}$$

2. Assume that no ambiguity exists and assign a whole cycle count ϕ_N to adjust the measured fraction to within ½ cycle of the predicted value:

$$\phi_O' = \phi_O + \phi_N$$

where ϕ_O' is defined as the observed phase.

C. CLOCK PHASE AND TIME ERROR CALCULATIONS

1. Subtract the observed from the predicted phase to compute the *phase* error of the local clock:

$$E_\phi = (\phi_{P_{(H \, or \, E)}} - \phi_O') \pm \phi_T = \Delta\phi \pm \phi_T$$

where ϕ_T represents the ambiguity as an integral number of carrier frequency cycles.

2. Divide the clock phase error by the carrier frequency to compute the clock time or epoch error:

$$E_T = \frac{E_\phi}{f} = \Delta t \pm t_T$$

where t_T represents the ambiguity as an integral number of carrier frequency periods.

cycle resolution even though the error on either carrier was quite nominal. The problem
of differential prediction error when using multiple frequencies is most severe when the
frequencies are closely spaced. In such cases, the nominal prediction for one of the
carriers can be obtained by interpolation of tables from 10.2, 11.33, and 13.6 kHz, but
the prediction for the second should be adjusted so that the difference reflects not only
the nominal dispersion, but also any structural differences in the signals as can be assessed,
for example, by fullwave computation. An example of a full wave calculation for a 250
Hz difference frequency is given in Figure 7, which shows significant modal complexity
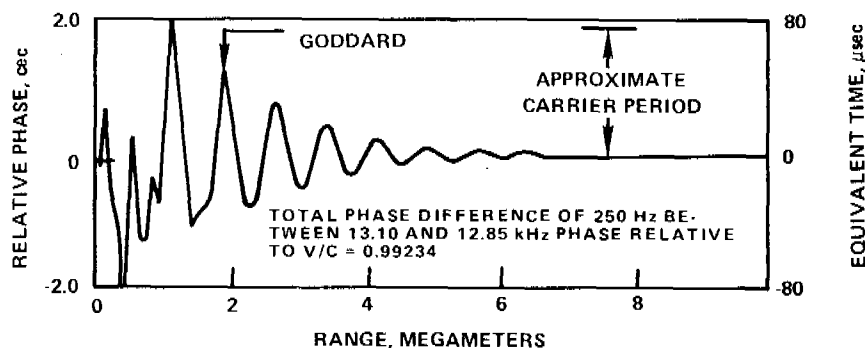to 4000 km during the day.

Figure 7. Relative phase of daytime OMEGA difference frequency, North Dakota to Goddard
(Wait's $\beta = 0.5$ km^{-1}, H' = 70 km profile).

CONCLUSIONS

Published OMEGA skywave corrections are easily applied to determine epoch or to account
for seasonal or diurnal phase variations when deducing frequency from 10.2 kHz
measurements.

ACKNOWLEDGEMENT

Credit is due Miss Pamela Mallory who wrote a desk-top computer program and prepared
the phasor sums shown in Figures 3, 4, and 5.

REFERENCES

1. E.R. Swanson and C.P. Kugel. "VLF Timing: Conventional and Modern Techniques
Including Omega." *Proceedings IEEE.*

2. E.R. Swanson, "Time Dissemination Effects Caused by Instabilities of the Medium." North Atlantic Treaty Organization Advisory Group for Aerospace Research and Development, Electromagnetic Wave Propagation Committee, *Phase and Frequency Instabilities in Electromagnetic Wave Propagation* K. Davies, ed. Slough England Technivision Services, 1970 (AGARD Conference Proceedings No. 33). pp. 181-98.

3. E.R. Swanson and W.R. Bradford. "Diurnal Phase Variation at 10.2 kHz." Naval Electronics Laboratory Center Technical Report 1781. August 11, 1971.

4. D.D. Crombie. "Periodic Fading of VLF Signals over Long Paths During Sunrise and Sunset." *Radio Science* 68D (1) (1964).pp. 27-34.

5. Richard A. Pappert and Floyd P. Snyder. "Some Results of a Mode Conversion Program for VLF." *Radio Science,* 7 (no. 10, October 1972). pp. 913-24.

6. E.R. Swanson, "VLF Phase Prediction." *VLF Propagation: Proceedings from the VLF Symposium.* G. Bjontegaard, Norwegian Institute of Cosmic Physics Report 7201. (January 1972). pp. 8-1 to 8-36.

7. J.R. Wait and K.P. Spies. *Characteristics of the Earth-Ionosphere Waveguide for VLF Radio Waves.* NBS Technical Note 300.

8. F.P. Snyder and R.A. Pappert. "A Parametric Study of VLF Modes Below Anisotropic Ionospheres." *Radio Science*, 4 (no. 3, March 1969). pp. 213-26.

9. E. R. Swanson and C. P. Kugel. "Omega VLF Timing." Naval Electronics Laboratory Center Technical Report 1740 (also NASA S-51743A-G, revision 1, 1972).

10. J. Wilson, J. Britt, and A. Chi. "Omega Timing Receiver, Design and System Test." PTTI *Proceedings.* 1972.